

Excited-state phase transition leading to symmetry-breaking steady states in the Dicke modelRicardo Puebla,¹ Armando Relaño,² and Joaquín Retamosa¹¹*Grupo de Física Nuclear, Departamento de Física Atómica, Molecular y Nuclear, Universidad Complutense de Madrid, Av. Complutense s/n, 28040 Madrid, Spain*²*Departamento de Física Aplicada I and GISC, Universidad Complutense de Madrid, Av. Complutense s/n, 28040 Madrid, Spain*
(Received 22 October 2012; published 19 February 2013)

We study the phase diagram of the Dicke model in terms of the excitation energy and the radiation-matter coupling constant λ . Below a certain critical value λ_c , all the energy levels have a well-defined parity. For $\lambda > \lambda_c$ the energy spectrum exhibits two different phases separated by a critical energy E_c that proves to be independent of λ . In the upper phase, the energy levels have also a well-defined parity, but below E_c the energy levels are doubly degenerated. We show that the long-time behavior of appropriate parity-breaking observables distinguishes between these two different phases of the energy spectrum. Steady states reached from symmetry-breaking initial conditions restore the symmetry only if their expected energies are above the critical. This fact makes it possible to experimentally explore the complete phase diagram of the excitation spectrum of the Dicke model.

DOI: [10.1103/PhysRevA.87.023819](https://doi.org/10.1103/PhysRevA.87.023819)

PACS number(s): 42.50.Nn, 05.30.Rt, 11.30.Qc, 64.70.Tg

I. INTRODUCTION

The rapid development of experimental techniques controlling ultracold atoms has given rise to a great breakthrough in the physics of quantum many-body systems. A logical outcome has been the increase of the interest in certain phenomena, such as nonequilibrium dynamics and quantum phase transitions (QPT's). In addition, it has entailed the revival of well-known physical models such as that formulated by Dicke, which describes the interaction between an ensemble of two-level atoms with a single electromagnetic field mode, as a function of the radiation-matter coupling [1]. Its most representative features are a second-order QPT, which leads the system from a normal to a superradiant phase, characterized by a macroscopic population of the upper atomic level [2], the emergence of quantum chaos, and the spontaneous symmetry breaking [3,4]. Although this model has been extensively studied from many points of view, there still exists a heated controversy about its significance in real physical systems. A no-go theorem was formulated in the 1970s, stating that the superradiant phase transition cannot occur in a general system of atoms or molecules interacting with a finite number of radiation modes in the dipole approximation [5]. In addition, it is not clear if this theorem also forbids the superradiant transition in other realizations of the Dicke model, as in circuit QED [6]. On the contrary, this transition has been experimentally observed with a superfluid gas in an optical cavity, giving rise to a self-organized phase [7]. All of these facts have turned the Dicke model into a multidisciplinary hot topic, involving different branches of physics. As a consequence, there exists an intense theoretical research; a few representative examples concern nonequilibrium QPT's [8], thermal phase transitions in the ultrastrong-coupling limit [9], or equilibration and macroscopic quantum fluctuations [10].

In this paper we explore the phase diagram of the Dicke model as a function of two control parameters: the radiation-matter coupling constant λ and the energy E of its eigenstates. We show that the energy spectrum can be divided into three different sectors or phases separated by certain critical values λ_c and E_c . For $\lambda < \lambda_c$ we find that parity is a well-defined quantum number at any excitation energy. The situation is

rather different if $\lambda > \lambda_c$. Below a certain critical energy E_c all the energy levels of the system are doubly degenerated, and, as a consequence, the parity symmetry of each level can be broken. Above the critical energy E_c there are no such degeneracies and parity is again a good quantum number. We can say that beyond λ_c the excited energy levels up to energy E_c inherit some of the properties of the superradiant phase, characteristic of the ground state. Moreover, we obtain an estimation of the finite-size scaling exponent of the critical energy, which is compatible with the one obtained by Vidal and Dusuel for the ground-state energy around the critical coupling [11].

In the second part of the paper, we show that this phase diagram entails measurable effects in the long-time dynamics of certain observables. Indeed, if one prepares the system in a symmetry-breaking ground state of the superradiant phase and then abruptly changes the value of the coupling parameter, the symmetry of the final steady state remains broken if its energy is below E_c , while it is restored in the opposite case. As a consequence, parity nonconserving observables relax to steady values different from zero only if the energy of the nonequilibrium initial state is below the critical. This fact constitutes an unheralded characteristic of the Dicke model that can be accessible to experiments and shed some light over the current controversy about the relevance of the critical behavior of this model in real physical systems.

The paper is organized as follows. In Sec. II we present the Dicke model and summarize its main features. In Sec. III we study the complete phase diagram of this model, including the finite-size scaling exponent for the critical energy. In Sec. IV, we explore the dynamical consequences of this phase diagram, in particular the dynamical symmetry-breaking. Finally, conclusions are summarized in Sec. V.

II. THE DICKE MODEL

The Dicke Hamiltonian can be written as follows:

$$H = \omega_0 J_z + \omega a^\dagger a + \frac{2\lambda}{\sqrt{N}}(a^\dagger + a)J_x, \quad (1)$$

where a^\dagger and a are the usual creation and annihilation operators of photons, $\vec{J} = (J_x, J_y, J_z)$ is the angular momentum, with a pseudo-spin length $J = N/2$, and N is the number of atoms. The frequency of the cavity mode is represented by ω and the transition frequency by ω_0 . Finally, the parameter λ is the radiation-matter coupling. Throughout this paper, we take $\hbar = 1$, and $\omega = \omega_0 = 1$. The parity $\Pi = e^{i\pi(J+J_z+a^\dagger a)}$ is a conserved quantity, due to the invariance of H under $J_x \rightarrow -J_x$ and $a \rightarrow -a$ [3], and thus all the eigenstates are labeled with positive or negative parities. The system undergoes a second-order QPT at $\lambda_c = \sqrt{\omega\omega_0}/2$, which separates the so-called normal phase ($\lambda < \lambda_c$) from the superradiant phase ($\lambda > \lambda_c$) [2]. In the latter the ground state becomes doubly degenerated and parity can be spontaneously broken—because of the fluctuations, the system can evolve into one particular ground state without a well-defined parity [4].

It is important to note that the system has a finite number of atoms but infinite photons, reason why it is mandatory to set in numerical calculations a *cutoff* in the photon Hilbert space. The convergence of our results is tested, checking their stability against small increases of this *cutoff*.

III. PHASE DIAGRAM

A. Critical energy

As previously mentioned, two different phases, separated by λ_c , are found in the Dicke model at zero temperature. The normal phase, where parity is a well-defined quantum number, and the superradiant phase characterized by a degenerated ground state. A convenient method to see if this phenomenon is also present in excited states is to analyze the difference

$$\Delta E_i(\lambda, N) = \left| \frac{E_i^{\Pi=+1}(\lambda, N) - E_i^{\Pi=-1}(\lambda, N)}{E_i^{\Pi=+1}(\lambda, N)} \right| \quad (2)$$

between the i th excited states of both parity sectors $\Pi = \pm 1$. If ΔE_i is different from zero, the corresponding eigenstates have well-defined parity; if it is zero, they are degenerated and one can perform a rotation that mixes both parities. Results for $N = 40$ atoms are shown in Fig. 1. For $\lambda > \lambda_c$ there exists an abrupt change from $\Delta E_i \approx 0$ to $\Delta E_i > 0$ at a certain critical energy $E_c(\lambda, N)$. A quantitative estimate of this energy can be obtained as the first eigenvalue E_i for which $\Delta E_i > k_{\text{err}}$, where k_{err} is a given error bound. For all the results shown below we have set $k_{\text{err}} = 10^{-6}$; similar ones are obtained with different bounds.

Since the actual phase transition occurs in the thermodynamic limit, it is mandatory to infer how this critical line evolves as $N \rightarrow \infty$. The behavior of a system with a finite number of atoms is just a precursor of the true critical behavior, and therefore $E_c(\lambda, N)$ is just a finite-size estimate of the real critical energy $E_c(\lambda, \infty)$. In a standard thermal phase transition, the critical temperature $T_c(\infty)$ can be estimated from the finite-size precursors $T_c(N)$ by means of the finite-size scaling law $|T_c(N) - T_c(\infty)| \propto N^{-1/\nu}$. In analogy with this, it is reasonable to suppose that the critical energy scales in the same way, $|E_c(N) - E_c(\infty)| \propto N^{-\alpha(\lambda)}$, where the finite-size scaling exponent $\alpha(\lambda)$ can in principle depend on the coupling λ . However, a direct estimate of this exponent from numerics is very complicated. As only small systems

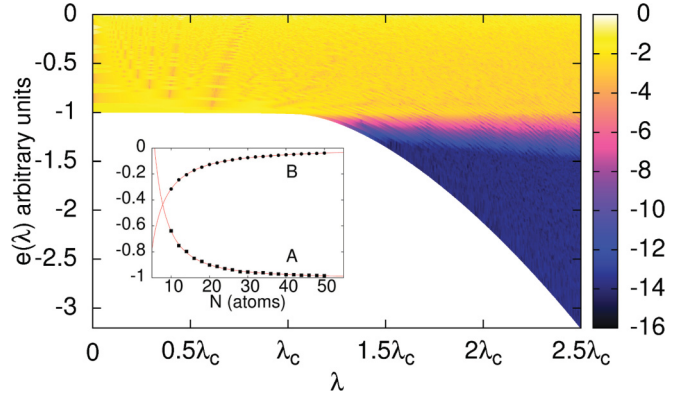


FIG. 1. (Color online) Intensity plot showing the decimal logarithm of the relative difference $\Delta E(E, \lambda, N)$ in terms of E/J and λ for a system with $N = 40$ atoms. Lighter regions (yellow online) correspond to the conserving-parity region, while darker regions (blue online) represents the spontaneously broken-parity phase. The inset shows the finite-size scaling of parameters A_N and B_N in Eq. (3).

(around 50 atoms) are accessible to the current computational capabilities, we observe quite large fluctuations which prevent a significative fit. These fluctuations are due to the fact that the level spacing around the critical energy is large, and therefore large “jumps” occur when changing λ and N . To solve this difficulty, we assume that for each value of N the critical line obeys the linear law

$$\frac{E_c(\lambda, N)}{J} = A_N + B_N \lambda, \quad \lambda > \lambda_c, \quad (3)$$

where the coefficients A_N and B_N are numerically determined by means of a least-squares fit. The results plotted in Fig. 1 support this assumption—it is clearly seen that the critical energy for $N = 40$ atoms behaves more or less linearly with λ . In any case, it is import to clarify that every point of this critical line is a set of critical points which are the precursors of excited-state quantum phase transitions (ESQPT's) for any $\lambda > \lambda_c$.

The inset of Fig. 1 displays the dependence of these coefficients on N . Solid circles represent the numerical points corresponding to B_N ; solid squares, the corresponding to A_N ; and solid lines the fits to power laws $N^{-\alpha}$. Numerical results are summarized in Table I. They are obtained by fitting the finite-size scaling to a law $f(N) = a + bN^c$. It is clearly seen that $A_N \rightarrow -1$ and $B_N \rightarrow 0$ as $N \rightarrow \infty$, and hence we conclude that $E_c(\lambda) = E_c(\lambda, \infty) = -J$. It is worth mentioning that this value coincides with that recently obtained in the study of the connection between an ESQPT and the development of quantum chaos and the critical decay of the survival probability [12,13].

TABLE I. Scaling law $f(N) = a + bN^c$ for coefficients A_N and B_N in Eq. (3).

	a	b	c
A_N	-1.0052 ± 0.0028	22.3 ± 2.4	-1.787 ± 0.048
B_N	0.0004 ± 0.0018	-6.28 ± 0.26	-1.300 ± 0.019

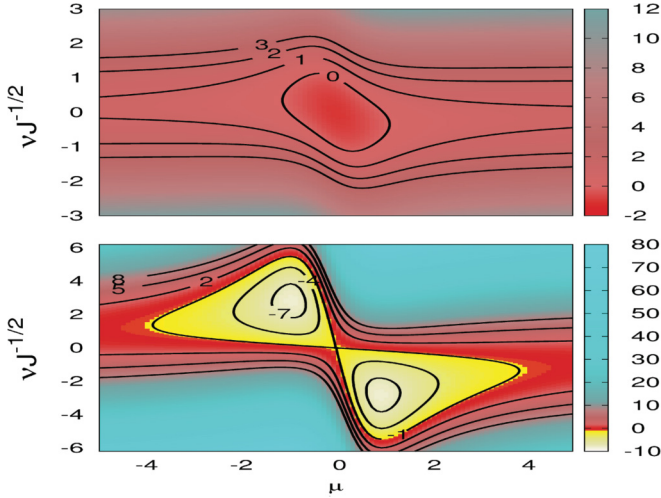


FIG. 2. (Color online) Contour plot of the energy surface $E_{\text{var}}(\mu, \nu, \lambda)/J$ for two different values of λ , one above and the other below the critical coupling λ_c . Upper panel $\lambda = 0.25$, lower panel $\lambda = 2.0$. Solid lines represent level curves.

We can also use the mean-field approximation, which gives the exact ground-state energy in the thermodynamic limit, to estimate $E_c(\lambda)$. Let us introduce for $\mu, \nu \in \mathbb{R}$ the coherent ansatz $|\mu, \nu\rangle = |\mu\rangle \otimes |\nu\rangle$, where

$$\begin{aligned} |\mu\rangle &= (1 + \mu^2)^{-J} e^{\mu J_+} |J, -J\rangle, \\ |\nu\rangle &= e^{\nu^2/2} e^{\nu a^\dagger} |0\rangle, \end{aligned} \quad (4)$$

correspond to the atomic and the photonic parts of the state, respectively. The resulting energy surface is

$$\begin{aligned} E_{\text{var}}(\mu, \nu, \lambda) &= \langle \nu, \mu | H | \nu, \mu \rangle = \omega_0 J \left(\frac{\mu^2 - 1}{\mu^2 + 1} \right) \\ &+ \omega \nu^2 + \lambda \sqrt{2J} \left(\frac{4\mu\nu}{\mu^2 + 1} \right). \end{aligned} \quad (5)$$

It is plotted in Fig. 2. The upper panel shows the case with $\lambda = 0.25$ (below λ_c), and the lower panel, the case with $\lambda = 2.0$ (above λ_c); in both panels a number of level curves are drawn with solid lines. The geometry of this surface reveals that the level curve $E = -J$ plays a special role. For $\lambda < \lambda_c$, it reduces to a single point at $(\mu, \nu) = (0, 0)$, which is the absolute minimum of the energy surface; for $\lambda > \lambda_c$, it changes to a nonanalytic level curve containing a saddle point. Moreover, the shape of the energy surface is quite different depending on whether E is below or above $E = -J$. In the former case, the energy surface exhibits two symmetric wells below $E = -J$, so that level curves are disjointed. On the contrary, for $E > -J$ there is just a single well with connected level curves for any value of λ . This behavior supports our previous numerical estimations for finite N , stating that $E_c(\lambda) = -J$. It is worth mentioning that this qualitative change of the level curves when crossing the critical energy $E = -J$ is fully compatible with the transition to chaos reported in Ref. [13] at the same energy. The disjointed and thus nonergodic level curves occur in the phase in which quantum chaos is not observed, whereas ergodic level curves appear in the quantum chaotic phase.

B. Finite-size scaling exponent

The scaling of the critical line found in the previous section can be used to estimate the finite-size scaling exponent $\alpha(\lambda)$. From the results of Table I, we can write $|E_c(\lambda, N) - E_c(\lambda, \infty)| \propto N^{-1.300}(22.3N^{-0.487} - 6.28\lambda)$. Therefore, for a large number of atoms N , the finite-size precursors of the critical energy scale as $|E_c(\lambda, N) - E_c(\lambda, \infty)| \propto N^{-1.300}$, and thus we can conclude that the finite-size scaling exponent is

$$\alpha(\lambda) = -1.300 \pm 0.019. \quad (6)$$

In view of this, we can state that the critical exponent is independent of the coupling constant λ and is therefore the same for every excited-state critical point. It worth mentioning that this result seems to be compatible with the value $\alpha = -4/3$ reported in Ref. [11] for the finite-size scaling exponent of the ground-state energy.

IV. DYNAMICAL SYMMETRY BREAKING

Baumann and co-workers [4] explored in real time the spontaneous parity breaking of the ground state at the superradiant phase transition, by measuring the behavior of $\langle J_x \rangle$ as the coupling constant λ increases in time and crosses the critical point. Here, we follow an analogous procedure to study the different phases of the excitation spectrum when $\lambda > \lambda_c$. We study the nonequilibrium dynamics and the relaxation to a steady state of certain physical observables, like J_x and $\hat{q} \equiv (a^\dagger + a)/\sqrt{2}$. They are physically measurable operators [4,14], which change the parity of the state on which they operate. Thus, they give rise to qualitatively different steady expectation values, depending on whether the energy of the nonequilibrium state is above or below E_c . Although we only report results for J_x , the behavior of \hat{q} is similar.

Let us take as our initial condition a symmetry-breaking ground state $|\Psi(0)\rangle = |\mu_i, \nu_i\rangle$, where (μ_i, ν_i) are the values that minimize the energy surface corresponding to a coupling constant λ_i inside the superradiant phase. Then we perform a *diabatic* change of λ , i.e., a quench $\lambda_i \rightarrow \lambda_f$, so that the initial state $|\mu_i, \nu_i\rangle$ is not an eigenstate of the final Hamiltonian $H(\lambda_f)$ anymore, but it becomes a nonequilibrium state. Its energy $E(\lambda_i, \lambda_f) = \langle \mu_i, \nu_i | H(\lambda_f) | \mu_i, \nu_i \rangle$ can be written as

$$\begin{aligned} E(\lambda_i, \lambda_f) &= -\omega_0 J \left(\frac{\lambda_i^2}{\lambda_i^2} \right) + 2J \frac{\lambda_i^4 - \lambda_c^4}{\omega \lambda_i^2} \\ &- 4J \frac{\lambda_f}{\lambda_i} \left(\frac{\lambda_i^4 - \lambda_c^4}{\omega \lambda_i^2} \right). \end{aligned} \quad (7)$$

The contours of $E(\lambda_i, \lambda_f)$ are shown in Fig. 3. It is clearly seen that choosing λ_i and λ_f properly, one can explore the different phases of the excited spectrum. In particular, from any initial condition being the ground state of the system with $\lambda_i \gtrsim 1.5\lambda_c$, both phases can be reached by just quenching the system to different final coupling parameters λ_f .

After performing the quench, we study the time evolution of $\langle J_x(t) \rangle = \langle \Psi(t) | J_x | \Psi(t) \rangle$, where $|\Psi(t)\rangle = e^{-iH(\lambda_f)t} |\Psi(0)\rangle$. If one expands the initial state in the eigenstate basis of $H(\lambda_f)$,

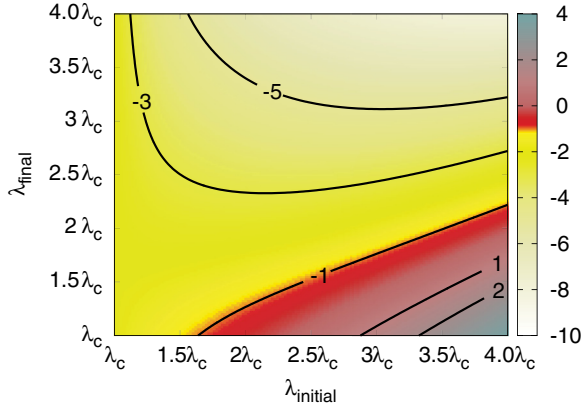


FIG. 3. (Color online) Contour plot of the energy surface $E(\lambda_i, \lambda_f)/J$ as a function of λ_i and λ_f . The critical energy line is placed at $E/J = -1$. The darker region (red online) corresponds to energies greater than the critical one, while the lighter zone (yellow online) corresponds to lower energies. Solid lines represent level curves.

denoted here as $\{|E_i\rangle\}$, the expectation value of J_x reads

$$\langle J_x(t) \rangle = \sum_{i,j} C_j^* C_i e^{-i(E_i - E_j)t} \langle E_j | J_x | E_i \rangle, \quad (8)$$

with $C_i = \langle E_i | \Psi(0) \rangle$.

Figure 4 displays, for a system with $N = 20$ atoms, the expected values $\langle J_x(t) \rangle$ after applying two different quenches. In the first quench $\lambda_i = 1.41$, $\lambda_f = 1.13$, and the energy $E(\lambda_i, \lambda_f)/J = -2.5$ is well inside the parity-breaking phase. It is clear seen that $\langle J_x(t) \rangle$ relaxes very quickly to a nonzero value. The same result is obtained in all the cases where the energy of the nonequilibrium state is $E(\lambda_i, \lambda_f) < -J$, although in this particular case, the time average $\langle J_x(t) \rangle < 0$, both positive and negative expectation values can be obtained. For every $\lambda_i > \lambda_c$ there are two degenerate ground states $|\pm\mu_i, \pm\nu_i\rangle$, characterized by values of μ and ν with opposite signs, that lead to different signs of $\langle J_x(t) \rangle$. The starting point of the second quench is also $\lambda_i = 1.41$, but the final

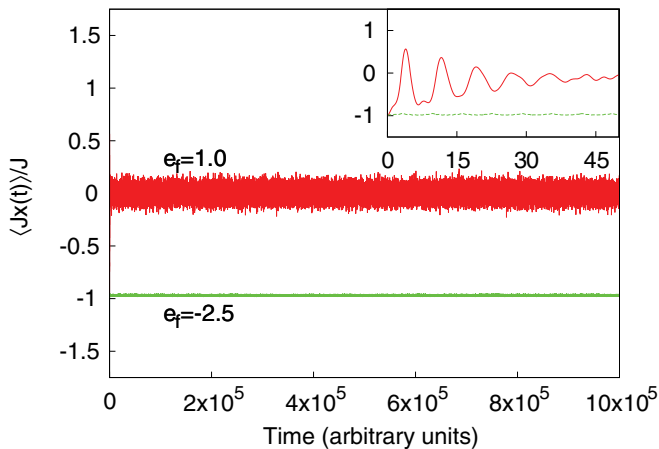


FIG. 4. (Color online) Time evolution of the expectation value of J_x for two different quenches and $N = 20$. The green line corresponds to a time evolution with $E < E_c$, and the red one to an evolution with $E > E_c$. The inset displays the evolution at shorter times.

coupling constant is reduced to $\lambda_f = 0.51$. The energy of the nonequilibrium state $E(\lambda_i, \lambda_f)/J = 1.0$ is now well above the critical energy. In this case, and in all where $E > E_c$, we obtain $\langle J_x(t) \rangle = 0$ in the steady state.

The physical explanation of this result is the following. For long enough time evolutions, almost any initial condition relaxes to a certain steady state around which it fluctuates [15]. Moreover, when the energy eigenvalues are not degenerated, the expectation values of any observable O in the steady state are given by the diagonal approximation $\langle O(t) \rangle \stackrel{t \gg 1}{\approx} \langle O \rangle_D = \sum_i |C_i|^2 \langle E_i | O | E_i \rangle$. On the contrary, if the energy eigenvalues are degenerated, the diagonal approximation does not hold, and thus it is possible that $\langle O(t) \rangle \stackrel{t \gg 1}{\not\approx} \langle O \rangle_D$. These are precisely the cases that we have found in our model. In the preserving-parity phase ($E > E_c$) one can apply the diagonal approximation because the energy levels are not degenerated. As parity is a good quantum number in this case, $\langle E_i | J_x | E_i \rangle = 0$ for every energy level. Therefore, whenever $E > E_c$ we find that $\langle J_x(t) \rangle \stackrel{t \gg 1}{\approx} \langle J_x \rangle_D = \sum_i |C_i|^2 \langle E_i | J_x | E_i \rangle = 0$. On the contrary, in the broken-parity phase, the energy eigenvalues are doubly degenerated with opposite parities so that the diagonal approximation is not valid. Thus, one can find expectation values $\langle J_x(t) \rangle \stackrel{t \gg 1}{\not\approx} 0$ in this phase.

Consequently, the steady expected value of J_x provides a neat signature of the two phases of the excited spectrum whenever $\lambda > \lambda_c$. In fact, it acts like an order parameter of the ESQPT, as it is equal to zero if $E > E_c$, and different from zero if $E < E_c$. Therefore, it suffices to follow the long-time dynamics of a parity-changing operator to infer whether the energy of the initial state is above or below the critical energy. Furthermore, as this is already true for small values of N , finite precursors of this phase transition could be clearly observed in experiments. In particular, the setup used in Ref. [4] is a good candidate for covering this aim.

V. CONCLUSIONS

We have studied the phase diagram of the Dicke model in terms of the coupling constant λ and the energy E . Using numerical calculations and the mean-field approximation, we have found different phases in the excitation spectrum, separated by certain critical values E_c and λ_c , where the latter also defines the critical point of the superradiant transition of the ground state. For $\lambda < \lambda_c$ we find a single phase where parity is a well-defined quantum number. On the contrary, for $\lambda > \lambda_c$ there exists a critical energy $E_c = -J$, where the ESQPT's take place, such that below E_c all the energy levels of the system are doubly degenerated and composed of states with opposite parities. Furthermore, we present a numerical estimation of the finite-size scaling exponent for such ESQPT's. As a consequence of the doubly degenerated states, fluctuations can entail a spontaneous parity breaking—the system can evolve into a state without a definite value of the parity. In some sense the excited energy levels up to energy E_c inherit the properties of the ground state in the superradiant phase. This fact leads to measurable dynamical consequences. Starting from a symmetry-breaking ground state in the superradiant phase and abruptly changing the

coupling parameter λ , the relaxed expected value of certain observables, like J_x or q , is different from zero only if the energy of the nonequilibrium state is below E_c . This constitutes an unexpected feature of the Dicke model, which could be observed in experiments similar to that of Ref. [4].

We think that the results contained in this paper might shed some light about the significance of the critical behavior of the Dicke model in real physical systems.

ACKNOWLEDGMENTS

The authors thank Borja Peropadre for his valuable comments. R.P. thanks J. M. Udías for his financial support. This work is supported in part by Spanish Government grants for the research projects FIS2009-11621-C02-01, FIS2009-07277, and CSPD-2007-00042-Ingenio2010, and by the Universidad Complutense de Madrid Grant No. UCM-910059.

-
- [1] R. H. Dicke, *Phys. Rev.* **93**, 99 (1954).
 - [2] K. Hepp and E. H. Lieb, *Ann. Phys. (NY)* **76**, 360 (1973); Y. K. Wang and F. T. Hioe, *Phys. Rev. A* **7**, 831 (1973); H. J. Carmichael, C. W. Gardiner, and D. F. Walls, *Phys. Lett. A* **46**, 47 (1973).
 - [3] C. Emary and T. Brandes, *Phys. Rev. Lett.* **90**, 044101 (2003); *Phys. Rev. E* **67**, 066203 (2003).
 - [4] K. Baumann, R. Mottl, F. Brennecke, and T. Esslinger, *Phys. Rev. Lett.* **107**, 140402 (2011).
 - [5] K. Rzazewsky, K. Wodkiewicz, and W. Zakowicz, *Phys. Rev. Lett.* **35**, 432 (1975); K. Rzazewsky and W. Wodkiewicz, *Phys. Rev. A* **13**, 1967 (1976); J. M. Knight, Y. Aharonov, and G. T. C. Hsieh, *ibid.* **17**, 1454 (1978); I. Bialynicki-Birula and K. Rzazewsky, *ibid.* **19**, 301 (1979).
 - [6] P. Nataf and C. Ciuti, *Nature Commun.* **1**, 72 (2010); O. Viehmann, J. von Delft, and F. Marquardt, *Phys. Rev. Lett.* **107**, 113602 (2011).
 - [7] K. Baumann, C. Guerlin, F. Brennecke, and T. Esslinger, *Nature (London)* **464**, 1301 (2010).
 - [8] V. M. Bastidas, C. Emary, B. Regler, and T. Brandes, *Phys. Rev. Lett.* **108**, 043003 (2012).
 - [9] M. A. Alcalde, M. Bucher, C. Emary, and T. Brandes, *Phys. Rev. E* **86**, 012101 (2012).
 - [10] A. Altland and F. Haake, *N. J. Phys.* **14**, 073011 (2012).
 - [11] J. Vidal and S. Dusuel, *Europhys. Lett.* **74**, 817 (2006).
 - [12] P. Pérez-Fernández, P. Cejnar, J. M. Arias, J. Dukelsky, J. E. García-Ramos, and A. Relaño, *Phys. Rev. A* **83**, 033802 (2011).
 - [13] P. Pérez-Fernández, A. Relaño, J. M. Arias, P. Cejnar, J. Dukelsky, and J. E. García-Ramos, *Phys. Rev. E* **83**, 046208 (2011).
 - [14] K. Banaszek, C. Radzewicz, K. Wódkiewicz, and J. S. Krasinski, *Phys. Rev. A* **60**, 674 (1999); S. Deléglise, I. Dotsenko, C. Sayrin, J. Bernu, M. Brune, J. Raimond, and S. Haroche, *Nature (London)* **455**, 510 (2008).
 - [15] P. Reimann and M. Kastner, *New J. Phys.* **14**, 043020 (2012); A. J. Short, *ibid.* **13**, 053009 (2011).